

# Antibacterial and Photodegradative Properties of Metal Doped TiO<sub>2</sub> thin Films Under Visible Light

Jerneja Šauta Ogorevc,\* Elizabeta Tratar Pirc,  
Lev Matoh and Peter Bukovec

Faculty of Chemistry and Chemical Technology, University of Ljubljana, Aškerčeva 5, SI-Ljubljana, Slovenia

\* Corresponding author: E-mail: neja.sauta@fkt.uni-lj.si

Received: 06-07-2011

## Abstract

Doped (Au, Ag) and undoped TiO<sub>2</sub> thin films were prepared on soda-lime glass via the sol-gel method by dip-coating from TiCl<sub>4</sub> precursor, followed by 30 minutes calcination at 500 °C to obtain transparent thin films with good adhesion to the substrate. XRD analysis showed that the particle size of samples heat treated at 500 °C was ~10 nm for all of the samples prepared, both doped and undoped ones. SEM images revealed that the thin film surface was homogeneous and nano-porous. The hydrophilicity of the thin films was estimated by contact angle measurements. The photodegradation rate of an aqueous solution of the azo dye Plasmocorinth B on the thin films was tested by in-situ UV-Vis spectroscopic measurements of the dye solution. The best photocatalytic activity under visible and UVA light was exhibited by undoped TiO<sub>2</sub> thin films, whereas Au doped thin films were slightly less active. On the other hand, the best antimicrobial activity toward the *E. coli* strain DH5α under visible light was displayed by the Au/TiO<sub>2</sub> thin films.

**Keywords:** Photodegradation, photokilling, TiO<sub>2</sub> thin films, doping, UV/Vis spectroscopy

## 1. Introduction

The purification of water by semiconductor photocatalysis is a rapidly growing area of interest for both research workers and water purification companies.<sup>1</sup> Titanium dioxide is widely used as a semiconductor photocatalyst because of its long-term stability to UV light and water, the absence of toxicity and its good photocatalytic activity.

A variety of methods have been developed to prepare TiO<sub>2</sub> thin films, of which the sol-gel method and the dip-coating technique are the most widely used. These processes are relatively cheap, and enable deposition on various substrates. Using this technique TiO<sub>2</sub> films of high photocatalytic activity have been produced.<sup>2–4</sup>

TiO<sub>2</sub> photocatalyst is mostly used in powder form, where the final step of the photocatalytic process is a particle-fluid separation for catalyst recycling, which is not only inconvenient but also time consuming, expensive and almost impossible on a large scale. On the other hand, immobilization of TiO<sub>2</sub> on rigid supports reduces its photocatalytic activity since the reaction occurs at the liquid-solid

interface and only a part of the catalyst is in contact with the reactant.

TiO<sub>2</sub> absorbs only 3–5% of the energy of the solar spectrum, which is why numerous studies have been performed to extend the photoresponse.<sup>5–7</sup>

Many variables affect the photoactivity of the TiO<sub>2</sub> photocatalyst such as particle size, surface area,<sup>8–10</sup> crystal structure and the method of particle preparation, temperature of reaction, incident light intensity,<sup>11</sup> pH of solution<sup>12,13</sup> and catalyst loading. Crystal structure and particle size<sup>14</sup> are particularly important factors in determining photoactivity; anatase titania nanoparticles have a higher activity than rutile ones.<sup>15–17</sup>

The mechanism of the photocatalyst process has been extensively described in the literature and several complex reaction pathways have been reported.<sup>18–21</sup> The photocatalytic process in anatase TiO<sub>2</sub> particles includes chemical steps that produce highly reactive species. On irradiation of TiO<sub>2</sub> with photons of wavelength ≤385 nm, an electron is promoted from the valence band to the conduction band, thus forming an electron-hole pair.<sup>22</sup> The photogenerated holes and electrons react with water molecules attached to the TiO<sub>2</sub> surface in the presence of oxy-

gen to form hydroxyl radicals ( $\cdot\text{OH}$ ). These are highly reactive in the oxidation of organic substances and the inactivation of bacteria and viruses.<sup>21,23</sup>

Surface modification by doping with metal ions and organic polymers has been proven to be an efficient route for improving the separation of photo-produced electron-hole pairs, which results in enhancement of the photocatalytic activity of  $\text{TiO}_2$ .<sup>24</sup> Doping with noble metals allows extending the light absorption of large band gap semiconductors to the visible range.

Some authors also reported enhanced photoactivity of nanocomposite  $\text{TiO}_2$  thin films, when the percentage of metal is around 10 wt%.<sup>25</sup>

It has been reported by Matsunga et al. that  $\text{TiO}_2$  photocatalysts are also effective antibacterial agents under UV light.<sup>26</sup> Their work showed that  $\text{TiO}_2$  particles were effective in sensitizing the photokilling of bacteria such as *Lactobacillus acidophilus* and *Escherichia coli* (*E. coli*). Fujishima et al. have reviewed the antibacterial effects and detoxifying actions of  $\text{TiO}_2$  photocatalyst and found that titanium dioxide photocatalyst was more effective than any other related antibacterial agent tested.<sup>27</sup>

From this perspective, the purpose of the present work was to prepare  $\text{TiO}_2$  thin films doped with Ag and Au (1 wt%) and to test their photocatalytic activity under UV and visible light. The photoefficiency of the thin films was determined by *in-situ* UV-Vis spectroscopic measurements of the decolourisation of the azo dye Plasmocorinth B which is stable under UVA light in the absence of a photocatalyst. The design and utilisation of a reactor with a home-made cell is described in detail, since reactor design plays an important role in photocatalytic treatment. A special holder for thin films on substrates was designed to achieve a maximal photocatalyst surface to volume of azo-dye solution ratio.

The majority of the work related to  $\text{TiO}_2$  has focused on UV light irradiation; only a few papers have demonstrated antibacterial efficacy in visible light.<sup>28</sup> Hence the objective of the present study was to investigate the photoinactivation of *E. coli* DH5 $\alpha$  using doped and undoped  $\text{TiO}_2$  thin films deposited on  $\text{SiO}_2$  coated glass substrates on irradiation with visible light.

## 2. Experimental

### 2. 1. Preparation of Sols and Doping Agents

A detailed description of sol preparation has already been published.<sup>31</sup> Reagents used in the preparation procedure were of analytical grade. 0.1 mol of titanium(IV) tetrachloride (Fluka) was dissolved in 3.4 mol of absolute ethanol (Fluka) and then 300 mL of deionised water was added. A 25% solution of ammonia (TKI) was added to the titanate acid solution until the pH value reached 9 (app. 5 mL). The precipitate was rinsed with deionised water and centrifuged several times until  $\text{Cl}^-$  ions could no

longer be detected. The gel was then dissolved in 25–30 mL of 30% hydrogen peroxide (Belinka) to get a transparent orange sol of the titanium peroxo complex. Finally the triblock copolymer Pluronic F127 (Sigma) was added directly to the sol (3 g of Pluronic F127 per 50 mL of sol), to enhance the porosity of the films. It was reported that addition of Pluronic enhances the photocatalytic activity of thin films.<sup>32</sup> The sol was diluted with water to obtain a viscosity suitable for deposition of films (approx. 80 cP). The resultant Ti-peroxo sol was stirred overnight before deposition of the films.

Two kinds of doped thin films were prepared; thin films doped with 1 wt% of gold and 1 wt% of silver.

A colloidal silver solution was prepared *in-situ* in the  $\text{TiO}_2$  sol as follows. 6.8 mg (1 wt%) of  $\text{AgNO}_3$  (Kemika) was added to 30 mL of the prepared  $\text{TiO}_2$  sol. Then 5 mL of a solution of ascorbic acid (8 mmol  $\text{L}^{-1}$ ) was added dropwise to achieve reduction of  $\text{Ag}^+$  to  $\text{Ag}^0$ .

After stirring for 30 minutes, the doped peroxo-sol was subjected to dialysis through a Sigma dialysis tubing membrane against water to eliminate counter ions from the sol.

Colloidal gold was prepared according to Turkevich *et al.*<sup>33</sup> 40  $\mu\text{mol}$  of  $\text{HAuCl}_4$  (Fluka) was dissolved in 19 mL of deionised water and then heated to boiling point. During heating and vigorous stirring 1 mL of 0.5% solution of sodium citrate (Sigma Aldrich) was added. The solution was stirred for the next 30 minutes and then distilled water was added. The red colloidal gold was added directly to the peroxo-sol so that the percentage of gold in the sol was 1 wt%.

From all the prepared sols, the corresponding xerogels were prepared by drying the sols in air at ambient temperature.

### 2. 2. Preparation of thin Films

Soda-lime glass plates (75 mm  $\times$  12 mm  $\times$  1 mm) were used for the deposition of films for photocatalytic experiments. For TG and DSC measurements thin films were deposited on aluminium foil. Thin films were also prepared on platinum foil in order to test the adhesion to various substrates. The plates were first cleaned thoroughly with ethanol and distilled water in an ultrasonic bath for 5 minutes and dried before deposition. A  $\text{SiO}_2$  protective layer ( $\sim$  150 nm) was deposited from a  $\text{SiO}_2$  sol which was prepared according to Černigoj *et al.*<sup>34</sup>

After deposition of the  $\text{SiO}_2$  layer, a wetting agent (1 wt% of Etholat  $\text{C}_{13}\text{H}_{27}\text{O}(\text{CH}_2\text{--CH}_2\text{--O})_6\text{--H}$  (Teol) in distilled water) was dispersed on the substrate to improve the adhesion of the  $\text{TiO}_2$  peroxo-sol. After dipping the substrate into the sol and pulling it out at a uniform pulling rate of 5 cm/min, the thin film was first dried in air at room temperature and then calcined at 500 °C. The thickness of the film was increased by repeating the dipping and heat-treatment cycles. Between two subsequent coatings, films were calcined for 15 minutes at 500 °C and af-

ter the last coating the calcination time was increased to 30 minutes. The same procedure was used for thin films prepared at 350 °C and 450 °C. The final number of layers was 4 for undoped and 6 for doped films.

### 2. 3. Characterization of Thin Films and Xerogels

The crystallinity of TiO<sub>2</sub> xerogels was identified using a PANalytical X'Pert PRO MPD diffractometer employing Cu K $\alpha$  radiation from 5 to 80° 2 $\theta$  in steps of 0.04° and a time per step of 1 s.

Thermoanalytical measurements were performed on a Mettler Toledo TG/SDTA 851° instrument. During dynamic measurements, the temperature ranged from room temperature up to 900 °C for the xerogels with a heating rate of 5 K/min. Differential scanning calorimetry (DSC) measurements were made with a Mettler Toledo DSC 822° instrument. Platinum crucibles were used for TG measurements and aluminium crucibles for DSC measurements. The baseline was subtracted in all cases. Xerogel intermediates used for Fourier transform infrared (FT-IR) spectroscopy and X-ray diffraction (XRD) analyses were prepared by dynamic TG measurements up to the chosen temperature.

FT-IR spectroscopic measurements were made using a Perkin Elmer System 2000 spectrophotometer with a resolution of 4 cm<sup>-1</sup>. KBr pellets embedded with xerogel intermediates were prepared for this purpose.

The mass of TiO<sub>2</sub> deposited was estimated by weighing the substrate before and after deposition and calcination. The concentration of Ti<sup>4+</sup> in the sol was determined using the gravimetric method. 5 mL of sol was dried in air at ambient temperature and calcined at 900 °C for 30 minutes. The remained TiO<sub>2</sub> powder was weighed and the mass concentration calculated. Using the TiO<sub>2</sub> concentration in the sol, the wt% of the dopants was then calculated.

The surface hydrophilicity of thin films on SiO<sub>2</sub>-coated soda-lime glass was studied in ambient air at room temperature using a horizontal microscope with a protractor eyepiece. For this purpose, a Contact Angle Meter (CAM-100), KSV Instruments Ltd, Finland, was used.

A Zeiss Supra 35VP field emission scanning microscope (SEM) equipped with an Inca 400 energy dispersive spectroscope (Oxford Instruments) was used to study the surface of thin films deposited on soda-lime glass covered with a SiO<sub>2</sub> protective layer and to estimate their thickness. Thin films were covered with carbon to provide suitable conductivity of the sample.

### 2. 4. Photocatalytic Cell and Photoreactor

The cell consisted of a glass tube with an inner diameter of 4 cm. The glass tube contained a Teflon holder for 8 glass slides with the immobilized catalyst surrounding a metal tube used for purging with oxygen (Figure 1).

There was a gap of approximately 2 mm between the glass slides and the tube, which enabled homogeneous mixing of the solution in the cell. The effective volume of the cell was 90 mL.

The cell was inserted into the reactor with 6 lamps; a Hg Philips (360 nm) for UVA light and a Osram daylight (380–700 nm) for simulating visible light. Each lamp had an intensity of 15 W. The photoreactor had a ventilator to keep the temperature in the reactor at constant room temperature.

A fibre optic probe was dipped into the solution and coupled with a Varian Cary 50 UV-Vis spectrophotometer. The probe enabled *in-situ* UV-Vis spectroscopic absorbance measurements every 15 minutes. The azo dye solution in the cell was constantly purged with oxygen to ensure a high concentration on the thin film surface.

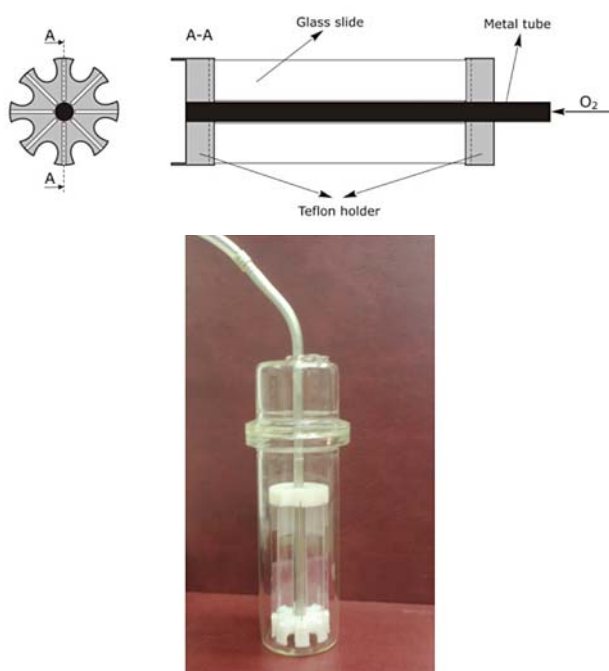


**Figure 1.** Scheme of a glass-slides holder (above) and a photo of the photocatalytic cell with holder and glass plates inserted (below).

### 2. 5. Photokilling Activity

The photokilling activity of doped and undoped TiO<sub>2</sub> thin films was evaluated under UVA and visible light as follows. *E. coli* cells (DH5 $\alpha$  strain) were precultured in 5 mL of nutrient broth at 36 °C overnight, and then washed by centrifuging at 4000 rpm. The treated cells were then re-suspended and diluted to ~10<sup>5</sup> colony forming units (CFU)/mL with 0.9% NaCl. The diluted cell suspension was pipetted onto an Au/TiO<sub>2</sub>, Ag/TiO<sub>2</sub> or TiO<sub>2</sub> coated glass plate and illuminated with two Osram daylight bulbs (380–700 nm), or two UVA Philips Hg lamps,

for 90 minutes. After being illuminated, the cell suspension was collected in 0.9% saline solution. An appropriate dilution of the collected cells was incubated at 36 °C for 24 h on a nutrient agar medium to determine the number of viable cells in terms of the CFU. To investigate the effect of illumination on the bacteria, the whole procedure was repeated in the dark. The surviving colonies were counted by eye with the help of a magnifying glass and the bacterial survival was calculated according to the following formula (Eq. 1):

$$\text{bacterial survival (\%)} = \frac{N_{ref}}{N_{exp}} 100 \% \quad (1)$$

where  $N_{ref}$  is the live number of bacterial cells in the reference group and  $N_{exp}$  is the live number of bacterial cells in the experimental group.

### 3. Results and Discussion

The thin films were all transparent, uniform and had good adhesion to all of the tested substrates.

The primary sol remained transparent and stable for months if kept in a refrigerator; no coagulation or precipitate appeared. Doped sols kept in a refrigerator were stable for a week, then coagulation appeared. The concentration of  $Ti^{4+}$  in the sol was determined using the gravimetric method and found to be 5.6 mg/mL of sol.

#### 3.1. Surface Roughness and Morphology

To observe differences in film morphologies, AFM and SEM images were taken. The AFM image of an undoped thin film prepared from the  $TiO_2$  sol with no addition of Pluronic F127 revealed that surface roughness was about 6 nm (Figure 2 (left)). The SEM image of the undoped thin film revealed a homogenous and smooth surface (Figure 2 (right)).

The thin films made from doped sols were thinner due to dilution of the primary sol. For this reason, six-lay-

ered doped films were prepared to achieve comparable thicknesses of the films, which were estimated by SEM and are shown in Table 1.

**Table 1.** Thin film thicknesses and masses of thin films per  $cm^2$  of substrate

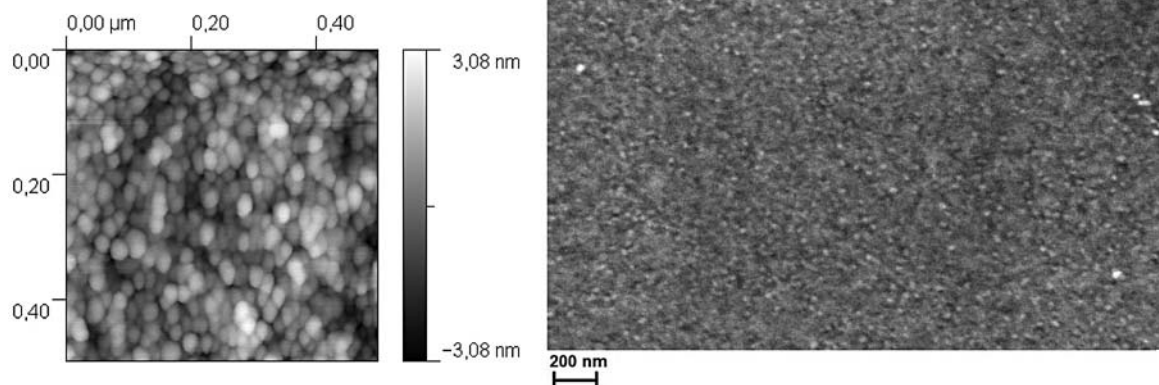
Thin film sample	Number of depositions	$TiO_2$ mass per unit of substrate area ( $mg/cm^2$ )	Thin film thickness (nm)
$TiO_2$	4	0.14	$160 \pm 10$
$TiO_2/Au$	6	0.12	$145 \pm 10$
$TiO_2/Ag$	6	0.12	$140 \pm 10$

Figure 3 shows AFM and SEM images of a calcined four-layered undoped  $TiO_2$  and of six-layered Au and Ag doped thin films on soda-lime glass with a  $SiO_2$  support. The AFM results revealed that surface roughness were pretty much the same for all of the prepared films: for Au doped thin films  $15.7 \pm 1.0$  nm,  $13.9 \pm 1.0$  nm for Ag doped and  $17.1 \pm 1.0$  nm for undoped thin films. Addition of the organic surfactant increased the surface roughness by about 10 nm.

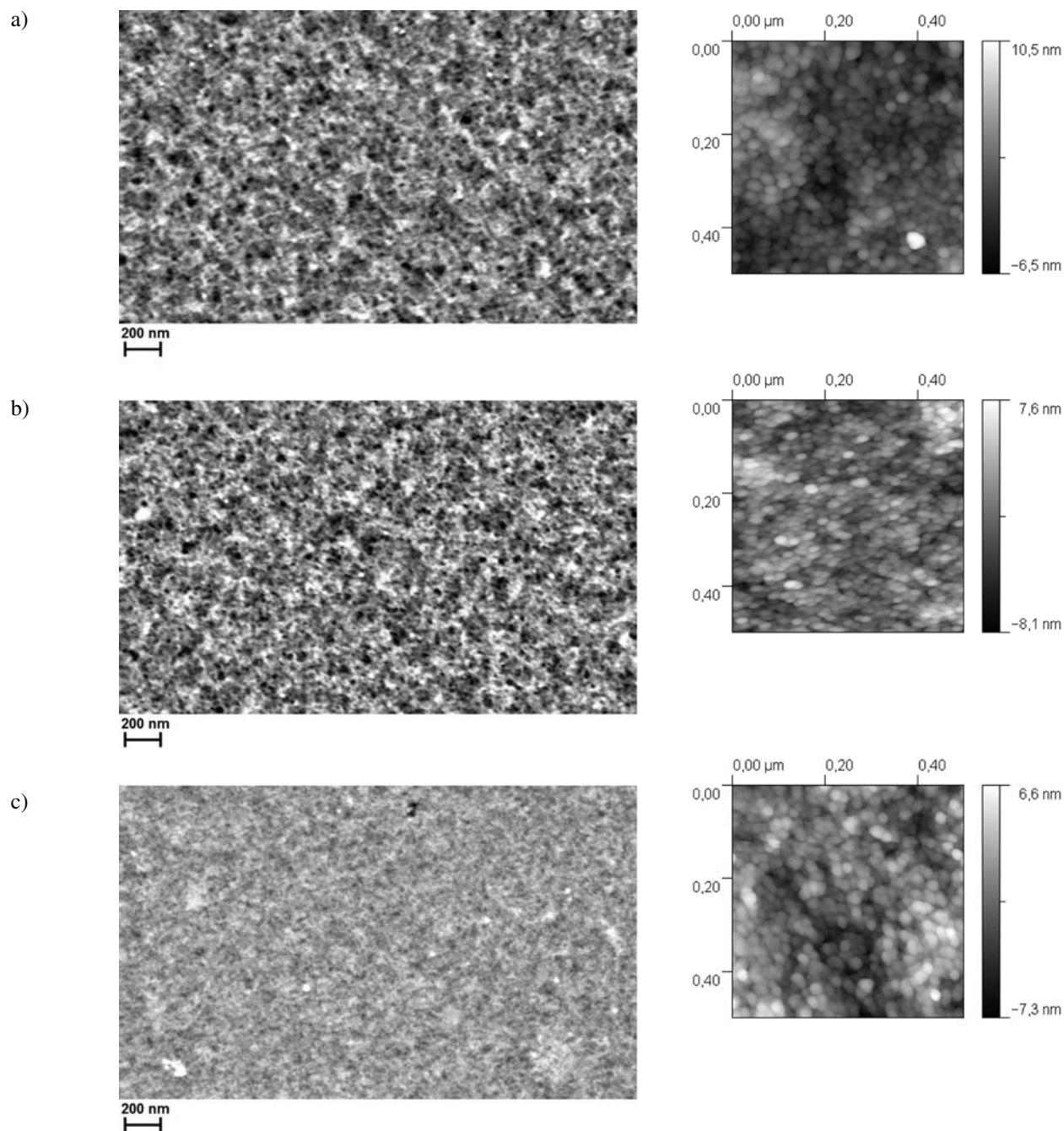
SEM images showed that the surface of the films was homogeneous and smooth, and that all of the prepared thin films were porous on the nano-level. SEM images of undoped and Au doped thin films showed higher porosity than the Ag doped thin film. Furthermore, undoped and Au doped thin films have a slightly greater surface roughness than the Ag doped thin film (AFM), which could explain the lower photocatalytic activity of the Ag doped thin film.

#### 3.2. Thermal Behaviour

Although thermal analysis of thin films is a demanding procedure and direct measurements are still not very common<sup>29</sup>, we succeeded in performing thermogravimet-



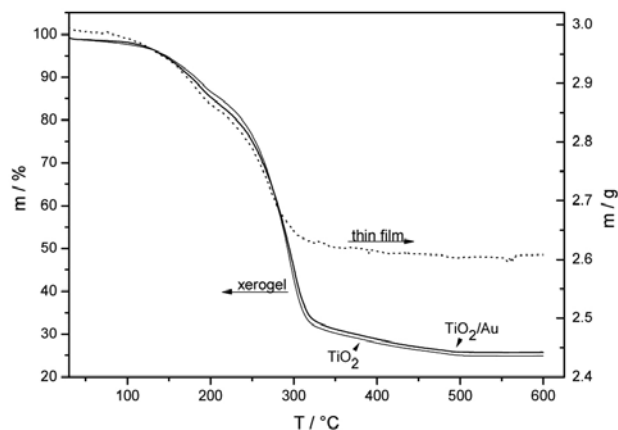
**Figure 2.** AFM (left) and SEM (right) images of  $TiO_2$  thin film made from sol without addition of Pluronic F127.



**Figure 3.** SEM (left) and AFM (right) images of (a)  $\text{TiO}_2$ , (b)  $\text{Au/TiO}_2$  and (c)  $\text{Ag/TiO}_2$  thin films deposited on a  $\text{SiO}_2$  support on soda-lime glass.

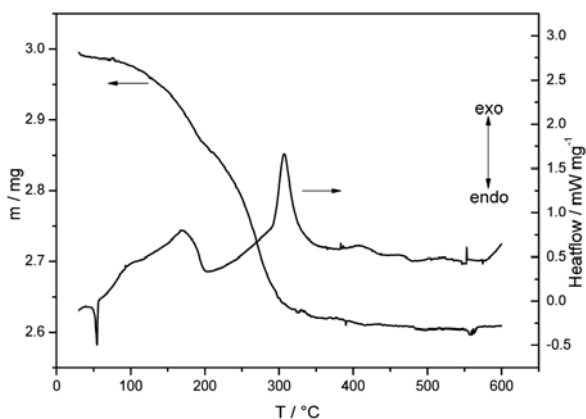
ric and DSC measurements of the thin films deposited on aluminium foil (temperature range from 25 to 600 °C). Comparison of TG measurements for  $\text{Au/TiO}_2$  thin films and the corresponding xerogels showed that the thermal decomposition curves were nearly the same, with onset temperatures at 119 °C and endset at 337 °C (Figure 4). The TG curve for the undoped  $\text{TiO}_2$  xerogel is identical to the doped  $\text{Au/TiO}_2$  xerogel. The same is true for the  $\text{Ag/TiO}_2$  samples (not shown in the graph for the sake of clarity).

Figure 5 presents TG and DSC measurements of an  $\text{Au/TiO}_2$  thin film. The sharp peak in the DSC curve at 56 °C could be ascribed to the dehydration process. The low onset temperature is probably due to the thin layer of the sample. It is known that thermal decomposition of thin films often occurs at lower temperatures.<sup>29</sup> The thermal decomposition of titanium peroxide to oxide began at 100 °C, which is evident from the second step of the TG curve. The presence of peroxy groups was determined by IR spectroscopy. Crystallization from the amorphous state to



**Figure 4.** Comparison of TG curves for xerogels (Au/TiO<sub>2</sub> and TiO<sub>2</sub>) and Au/TiO<sub>2</sub> thin film on aluminium foil.

anatase (determined using XRD) occurred at 305 °C which is evident from the exothermic peak in the DSC curve.



**Figure 5.** TG and DSC curves for a TiO<sub>2</sub> thin film doped with Au, deposited on aluminium foil.

DSC curves for undoped and Ag doped samples are practically the same as for Au doped (not shown in Figure 5). Since the wt% of dopants is low, differences were not expected.

The thermally untreated undoped TiO<sub>2</sub> xerogel, dried in air at ambient temperature, showed the diffraction profile of an amorphous material with some weak peaks characteristic of anatase (Figure 6). Two sharp peaks found at 19° and 23° in the XRD pattern of untreated xerogels originate from the organic surfactant as confirmed by the XRD pattern of Pluronic F127. The crystalline phase of samples heat-treated from 350 to 600 °C was predominantly anatase, whereas the sample treated at 700 °C showed a weak peak characteristic of the rutile phase. This indicates that the anatase phase is stable up to 600 °C and the rutile phase starts to grow above this temperature. The crystalline phase of the sample treated at 900 °C is a mixture of anatase and rutile.

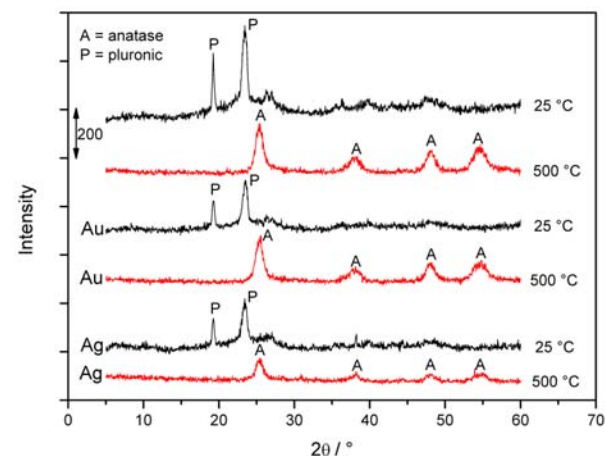
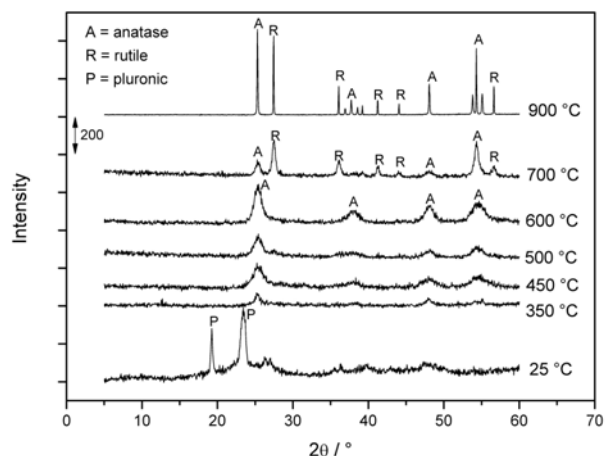


**Figure 6.** XRD patterns of undoped xerogels (top), and comparison of all of the prepared xerogels thermally treated at 25 and 500 °C (bottom).

The size of particles (calculated using the Scherrer equation) increased with increasing temperature. To ensure a small particle size, considering that the anatase phase is more active, and that soda-lime glass was used as a substrate, we chose 500 °C as an appropriate heating temperature for preparing the TiO<sub>2</sub> thin films as photocatalysts. The particle size of xerogels heat treated at 500 °C was ~10 nm for all the samples prepared, both doped and undoped. Thin films calcined at 350 °C and 450 °C for 30 minutes were less photocatalytically active than those calcined at 500 °C, which indicates that crystallization from the amorphous to the anatase phase was not complete at those temperatures. Consequently, the portion of anatase in the mixture was not high enough to act as an effective photocatalyst.

### 3. 3. Contact Angle Measurements

The interaction between the thin film surface and water was estimated by contact angle measurements. The change of the water contact angle was tested as a function of time during UV illumination (peak value at 355 nm)

with UVA radiation of an intensity of cca. 4 mW/cm<sup>2</sup> for both undoped thin films and thin films doped with Ag and Au. The results obtained are shown in Table 2 and confirmed the higher hydrophilicity of undoped thin films; the photoinduced hydrophilic property found indicates their self-cleaning ability.

**Table 2.** Water contact angles for TiO<sub>2</sub>, Ag/TiO<sub>2</sub> and Au/TiO<sub>2</sub> thin films as a function of time during UV illumination.

Contact angle (°)			
Illumination time (min)	TiO <sub>2</sub>	Ag/TiO <sub>2</sub>	Au/TiO <sub>2</sub>
0	61.0	67.1	69.4
10	40.9	56.4	51.0
20	27.5	37.5	38.0

### 3. 4. Photocatalytic Properties

Figure 7 shows the degradation curves (absorbances at 526 nm as a function of irradiation time) of the dye solution catalyzed by a four-layered (undoped) sample and six-layered thin films (Au and Ag doped) deposited on a SiO<sub>2</sub> support under UVA. Exposure time was 1 hour. The UV-Vis spectrum of Plasmocorinth B was recorded every 15 minutes.

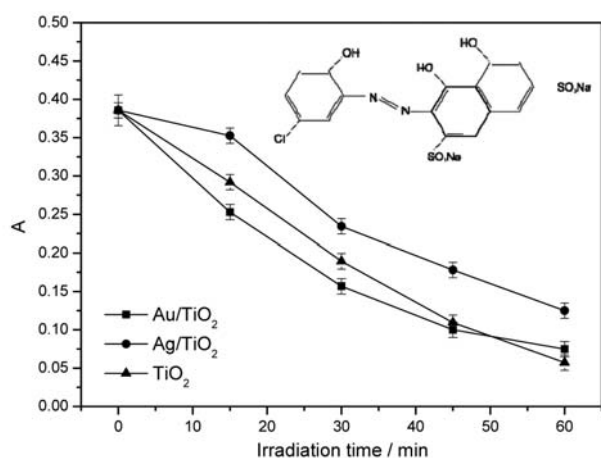


**Figure 7.** Photodegradation of Plasmocorinth B under UVA light and the formula of the azo-dye Plasmocorinth B.

The photodegradation curves indicate first-order kinetics, so all degradation curves were fitted as first-order reactions. The calculated mean half-lives and rate constants are listed in Table 3.

**Table 3.** Calculated half-lives and rate constants for photodecolourisation of an aqueous Plasmocorinth B solution (10 mg/L).

	TiO <sub>2</sub>	Ag/TiO <sub>2</sub>	Au/TiO <sub>2</sub>
Half-life (min)	38.6	127.4	40.7
Rate constant (min <sup>-1</sup> × 10 <sup>-3</sup> )	51.8	15.7	49.1

The best photocatalytic activity was displayed by undoped thin films (Fig 7 and Table 3). Au doped thin films were slightly less photoactive than undoped ones. But Ag doped thin films were much less active, which is also evident from the calculated half-life, which is 3-times longer than for the undoped thin film.

The photocatalytic activity of the thin films was also tested under visible light. In Fig. 8 decolourisation curves for undoped and Au doped thin films are shown. Ag doped thin films exhibited poor photocatalytic activity, and so the results are not presented in the figure.

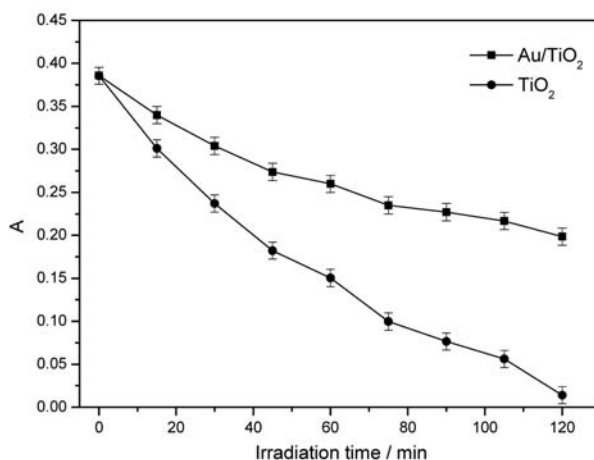


**Figure 8.** Photobleaching of Plasmocorinth B solution under visible light in contact with undoped and Au doped TiO<sub>2</sub> thin films.

According to the literature,<sup>30</sup> Au doped TiO<sub>2</sub> thin films were better photocatalysts than undoped ones, which is in contradiction to our results. Since the particle sizes and crystallinity are the same for both films, the poorer photocatalytic activity of doped films could be explained by the dopants playing the role of an electron trap. Due to the fact that doping elements act as trapping sites they can influence the life-time of charge carriers. Usually, they enhance the recombination of photogenerated electrons and holes, and therefore do not allow reaction to proceed with any noticeable effect under either ultraviolet or visible light.<sup>35,36</sup>

### 3. 5. Photokilling Activity

The number of viable bacterial cells did not decrease when the Au/TiO<sub>2</sub>, Ag/TiO<sub>2</sub> and TiO<sub>2</sub> coated substrates were stored in the dark and remained approximately 10<sup>5</sup> CFU/mL, the same as the blank sample. The same results were obtained when uncoated soda-lime glass was exposed to daylight illumination. Because the % of survival versus the illumination time for the coated and uncoated substrates exposed to UVA illumination was almost identical and within the range of error (5%), it is not possible to conclude that the bacteria were killed by TiO<sub>2</sub> and not by UVA illumination alone.

On the other hand, a great decrease in the number of viable cells was observed using an Au/TiO<sub>2</sub> film under daylight illumination (as shown in Figure 9), demonstrating its photokilling activity. When the initial cell concentration was ~10<sup>5</sup> CFU/mL, cell kill was complete within ~90 min under the described experimental conditions. It should be emphasized that the survival curve does not follow a simple single exponential decay process as a function of illumination time, but seems to consist of two steps, an initial step with a very low rate of photokilling, followed by a higher one.

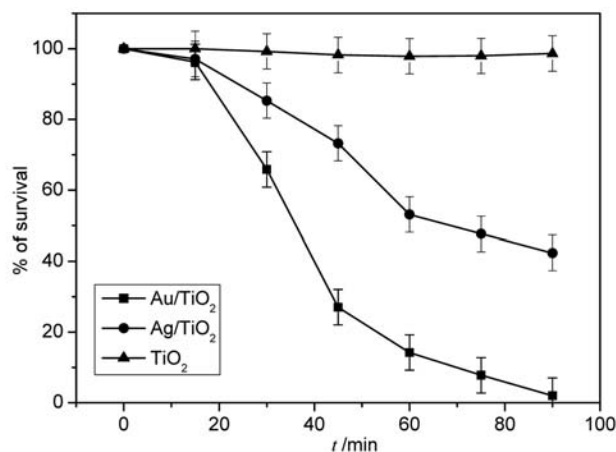


**Figure 9.** Plot of the survival of *E. coli* cells on TiO<sub>2</sub>, Ag/TiO<sub>2</sub>, Au/TiO<sub>2</sub> vs. illumination time under visible light.

Ag doped thin films demonstrated a slower activity, killing only about 50 % of the bacteria after 90 minutes. Undoped thin films showed negligible bactericidal activity under visible light.

## 4. Conclusion

The present paper describes the preparation of TiO<sub>2</sub> thin films doped with the noble metals silver and gold (1 wt%). The best photocatalytic activity was displayed by the undoped thin film (photodecolourisation half-life time 38.6 min). Au doped thin films were slightly less photoactive than undoped ones, whereas Ag doped thin films were much less active. TG, DSC and XRD analysis showed no differences between doped and undoped thin films. However, Au doped thin films evaluated under visible light on *E. coli* cells (DH5 $\alpha$  strain) showed a great decrease in the number of viable cells under daylight illumination, demonstrating its good photokilling activity. A possible explanation is that gold nano-particles catalyse the transfer of electrons to specific organic molecules which is enough to disable the bacterial cells, but insufficient to degrade the dye.

## 5. Acknowledgements

The authors would like to thank Dr. Irena Kozjek Škofic for SEM images.

## 6. References

1. A. Mills, R. H. Davies, D. Worsley, *Chem. Soc. Rev.* **1993**, 22, 417–425.
2. N. Negishi, K. Takeuchi and T. Ibusuki, *Appl. Surf. Sci.* **1997**, 121/122, 417–420.
3. L. Ge, M. X. Xu, M. Sun, *Mater. Lett.* **2006**, 60, 287–290.
4. R. S. Sonawane, S. G. Hegde, M. K. Dongare, *Mater. Chem. Phys.* **2002**, 77, 744–750.
5. M. Anpo, Y. Ichihashi, Takeuchi, H. Yamashita, *Stud. Surf. Sci. Catal.* **1999**, 121, 305–310.
6. H. Yamashita, M. Anpo, *Catal. Surv. Jpn.* **2004**, 8, 35–45.
7. A. Kudo, M. Sekizawa, *Chem. Comm.* **2000**, 15, 1371–1372.
8. P. A. Christensen, A. Dilks, T. A. Egerton, J. Temperley, *J. Mater. Sci.* **1999**, 34, 5689–5700.
9. P. A. Christensen, A. Dilks, T. A. Egerton, J. Temperley, *J. Mater. Sci.* **2000**, 35, 5353–5358.
10. T. Corrales, C. Peinado, N. S. Allen, M. Edge, G. Sandoval, F. Catalina, *J. Photochem. Photobiol. A: Chem.* **2003**, 156, 51–160.
11. Y. Ohko, K. Hashimoto, A. Fujishima, *J. Phys. Chem. A*, **1997**, 101, 8057–8062.
12. Kumar S, Davis AP, *Water Environ. Res.* **1997**, 69, 1238–1245.
13. A. C. van Dyk, A. M. Heyns, *J. Colloid. Interface Sci.* **1998**, 206, 381–391.
14. H. D. Jang, S. K. Kim, S. J. Kim, *J. Nanopart. Res.* **2001**, 3, 141–147.
15. R. R. Bacsa, J. J. Kiwi, *Appl Catal, B: Environ* **1998**, 16, 19–29.
16. V. Chabra, V. Pillai, B. K. Mishra, A. Morrone, D. O. Shah, *Langmuir* **1995**, 11, 3307–3311.
17. K. Hashimoto, A. Fujishima, T. Watanabe, *TiO<sub>2</sub> photocatalysis: Fundamentals and Applications* **1999**, BKC Inc, Japan.
18. X. X. Hu, C. Hu, J. H. Qu, *Appl Catal B: Environ* **2006**, 69, 17–23.
19. P. C. Maness, S. Smolinski, D. M. Blake, Z. Huang, E. J. Wolfrum, W. A. Jacoby, *App. and Environ. Microbiol.* **1999**, 65, 4094–4098.
20. Y. K. Kayano Sunada, K. Hashimoto, A. Fujishima *Environ. Sci. Tech.* **1998**, 32, 726–728.
21. Y. Kikuchi, K. Sunada, T. Iyoda, K. Hashimoto, A. Fujishima, *J. Photochem. Photobiol. A: Chem.* **1997**, 106, 51–56.
22. J. C. Harper, P. A. Christensen, T. A. Egerton, T. P. Curtis, J. Gunlazuardi *J. App. Electrochem.* **2001**, 31, 623–628.
23. A. Vohra, D. Y. Goswami, D. A. Deshpande, S. S. Block, *App Catal B: Environ* **2006**, 64, 57–65.
24. P. V. Kamat, *Chem. Rev.* **1993**, 93, 267–300
25. C. Yogi, K. Kojima, T. Hashishin, N. Wada, Y. Inada, E. D. Gaspera, M. Bersani, A. Martucci, L. Liu, T. K. Sham, *J. Phys. Chem. C* **2011**, 115, 6554–6560.

26. N. T. Matsunaga, R. Tomada, H. Wake, *FEMS Microbiology Letters*, **1985**, 29, 211–214.
27. K. Hashimoto, A. Fujishima, T. Watanabe, *TiO<sub>2</sub> Photocatalysis: Fundamentals and Applications*, BKC Inc., Japan, **1999**.
28. L. Caballero, K. A. Whitehead, N. S. Allen, J. Verran *J. Photochem. Photobiol. A: Chem.* **2009**, 202, 92–98.
29. R. Cerc Korošec, P. Bukovec, *Acta Chim. Slov.* **2006**, 53, 136–147.
30. R. S. Sonawane, M. K. Dongare, *J. Mol. Catal. A: Chem.* **2006**, 243, 68–76.
31. J. Šauta Ogorevc, U. Lavrenčič Štangar, P. Bukovec, *Acta Chim. Slov.* **2008**, 55, 889–896.
32. U. Lavrenčič Štangar, U. Černigoj, P. Trebše, K. Maver, S. Gross, *Monatsh. Chem.* **2006** 137, 647–655.
33. J. Turkevich, P.C. Stevenson, J. Hillier, *J. Phys. Chem.* **1953**, 57(7), 670–673.
34. U. Černigoj, U. Lavrenčič Štangar, P. Trebše, P. Rebernik Ribič, *Acta Chim. Slov.* **2006**, 53, 29–35.
35. Z. H. Yuan, J. H. Jia, L. Zhang, *Mat. Chem. Phys.* **2002**, 73, 323–326.
36. L. Palmisano, V. Augugliaro, A. Sclafani, M. Schiavello, *J. Phys. Chem.*, **1988**, 95, 6710–6713.

## Povzetek

Dopirane (z Ag in Au) in nedopirane tanke plasti TiO<sub>2</sub> smo pripravili iz prekursorja TiCl<sub>4</sub> po sol-gel postopku s tehniko potapljanja. Plasti smo žgali 30 minut pri temperaturi 500 °C in tako dobili tanke plasti z dobro oprijemljivostjo na steklo. XRD analiza je pokazala, da je velikost delcev žganih pri 500 °C ~10 nm za vse pripravljene vzorce; dopirane in nedopirane. Iz SEM posnetkov je razvidno, da je površina tankih plasti homogena in nanoporozna. Fotokatalitsko aktivnost smo ocenili z razgradnjo vodne raztopine azo barvila Plazmokorinta B, kar smo spremljali z *in-situ* UV-Vis spektroskopijo. Najbolj fotokatalitsko aktivne so bile nedopirane tanke plasti (pod vidno in UVA svetlobo), medtem ko so bile plasti dopirane z zlatom malenkost manj aktivne. Po drugi strani pa so plasti dopirane z zlatom pod vidno svetlobo izkazale najboljše protimikrobno delovanje na *E. coli* DH5α.